Relativistic photoionization with elliptically polarized laser fields in the ultra violet region

Tor Kjellsson Lindblom[1,2] and Sølve Selstø[1]

[1]*Faculty of Technology, Art and Design, OsloMet – Oslo Metropolitan University, NO-0130 Oslo, Norway*
[2]*PDC Center for High Performance Computing, KTH Royal Institute of Technology, SE-100 44 Stockholm, Sweden*

We study relativistic effects in photo ionization of a hydrogen atom exposed to an intense laser pulse of general ellipticity. The frequency of the laser pulse resides in the ultra violet region. To this end, the semi-relativistic approach introduced in T. Kjellsson Lindblom et al., Phys. Rev. Lett. **121**, 253202 (2018) is applied. We present in some detail how this approximation is derived from the Dirac equation for elliptically polarized light within the so-called *long wavelength approximation*. The validity of the semi-relativistic approach is confirmed by direct comparison with the solution of the Dirac equation. It is found that the total ionization yield depends very weakly on ellipticity in the case of ionization from the isotropic ground state. With the excited initial state $n = 2$, $\ell = m_\ell = 1$, however, pronounced ellipticity dependence is seen – in particular at the stabilization peak. Albeit small, relativistic corrections to the ionization probabilities are found. The correction is found to be largest for linear polarization. While relativistic effects tend to reduce the total ionization probability for most intensities considered, we also report a slight relativistic enhancement at comparatively modest field strengths.

I. INTRODUCTION

The theoretical and computational study of the interaction between matter and light is frequently conducted by solving the non-relativistic Schrödinger equation in the so-called *dipole approximation*, in which magnetic interactions are disregarded. However, in order to properly account for the physics involved in state of the art experiments with high laser intensities, this is no longer any fully adequate approach. With laser pulses available already now or in the near future [1–3], several interesting possibilities are opening, see, e.g., Ref. [4]. In order to describe these phenomena properly, the ability to describe the light-matter interaction in a relativistic framework which incorporates the magnetic field as well as the electric field is vital.

This is, however, hindered by several complications. The inclusion of magnetic interactions, e.g., preclude the convenient cylindrically symmetric description of the system. And the relativistic description provided by the Dirac equation introduces several aspects which complicates the numerical implementation. Examples of such are the inherent stiffness due to the mass energy term and the problem of so-called *spurious states* contaminating the spectrum of the numerical Hamiltonian.

Fortunately, we have seen several significant contributions for overcoming all of these obstacles in recent years. For instance, it has been demonstrated that magnetic interactions are conveniently incorporated within the so-called *propagation gauge* [5, 6]. When it comes to solving the time-Dependent Dirac equation, the so-called *generalized pseudospectral method* [7], and the method of Ref. [8], in which the *matrix iteration method* is applied, represent promising venues. As for spurious solutions, which frequently appear in the spectrum of the numerical representations of the Dirac Hamiltonian, several remedies are presented, see, e.g., Refs. [7, 9–11].

The present work is based on the semirelativistic formulation of the interaction presented in Ref. [12], which, in turn, is based on a relativistic formulation of the propagation gauge [13]. Also here we will explain how relativistic effects in the softly relativistic region may be accounted for by substituting the rest mass in the dynamical equation with an effective field-dressed mass. This allows for a relativistic description of the dynamics within the framework of a slightly modified Schrödinger equation. Not only does this evade the complications inherent to the numerical solution of the time-dependent Dirac equation; it also allows us to *analyse* the resulting quantum state by more familiar and technically simpler means than those pertaining to the relativistic four-component wave function.

In Ref. [12] the derivation of this semirelativistic method was outlined from three different starting points: from the classical Hamiltonian function, from the relativistic Klein-Gordon equation and from the Dirac equation. In this work we will review the latter derivation in more detail. And we will do so for external laser fields with general ellipticity. This external field is assumed to be independent of spatial variables. While this appears to be a rather restrictive approximation, it does include the leading magnetic interaction for strong fields. This is owing to the fact that the interaction is formulated in the propagation gauge in the first place.

The resulting effective semirelativistic Hamiltonian is derived in the next section. In addition to the semi-relativistic method, we have also solved the fully relativistic and non-relativistic equations. We have done so in order to validate the accuracy of the semi-relativistic approach and in order to identify relativistic corrections. Correspondingly, in Sec. II we also briefly outline how the numerical solutions of these dynamical equations are implemented. In Sec. III we present and analyse our results, while we summarize our findings in Sec. IV. Atomic units (a.u.), defined by choosing $\hbar$, the elementary charge e, the electron mass m and $4\pi\varepsilon_0$ as the unit of their respective quantities, are applied where stated explicitly. This only applies to numerical parameters, not to any general equations.

Tor Kjellsson Lindblom and Sølve Selstø. Relativistic photoionization with elliptically polarized laser fields in the ultraviolet region
Phys. Rev. A 104, 043102 (2021). DOI: https://doi.org/10.1103/PhysRevA.104.043102

II. THEORY

We take the external, spatially dependent electromagnetic field to be given by a vector potential of form

$$\mathbf{A}(\eta) = \frac{E_0}{\omega} f(\eta) \big[\hat{\mathbf{a}}_1 \sin\delta \sin(\eta+\phi) + \hat{\mathbf{a}}_2 \cos\delta \cos(\eta+\phi)\big], \tag{1}$$

where the variable

$$\eta = \omega t - \mathbf{k}\cdot\mathbf{r} = \omega(t - \hat{\mathbf{k}}\cdot\mathbf{r}/c). \tag{2}$$

The unit vectors $\hat{\mathbf{k}}$, $\hat{\mathbf{a}}_1$ and $\hat{\mathbf{a}}_2$ constitute a right-handed coordinate system. The former is the propagation direction and the latter two are orthogonal polarization directions. As the propagation direction $\hat{\mathbf{k}}$ is orthogonal to $\mathbf{A}$ at all times, the field satisfies the Coulomb gauge restriction, $\nabla\cdot\mathbf{A} = 0$. The parameter δ determines ellipticity; the field is circularly polarized for $\delta = \pm 45^\circ$ and linearly polarized for $\delta = 0$, and the envelope function f is typically slowly varying during one optical cycle $2\pi/\omega$. The phase ϕ is the so-called carrier envelope phase.

The time-dependent Dirac equation may be written

$$i\hbar\frac{d}{dt}\Psi = H\Psi \quad , \tag{3}$$

where the Hamiltonian is usually given in terms of minimal coupling,

$$H_{\rm mc} = c\boldsymbol{\alpha}\cdot[\mathbf{p} + e\mathbf{A}] + mc^2\beta + V, \tag{4}$$

where $V(\mathbf{r})$ is the Coulomb potential, which may correspond to a bare point charge or to some other effective potential. We adopt the usual representation in terms of Pauli matrices for $\boldsymbol{\alpha}$,

$$\boldsymbol{\alpha} = \begin{pmatrix} 0 & \boldsymbol{\sigma} \\ \boldsymbol{\sigma} & 0 \end{pmatrix} \tag{5}$$

and

$$\beta = \begin{pmatrix} \mathbb{1}_2 & 0 \\ 0 & -\mathbb{1}_2 \end{pmatrix} \quad . \tag{6}$$

The wave function of the Dirac equation is a four-component bi-spinor,

$$\Psi_{\rm R} = \begin{pmatrix} \Phi \\ X \end{pmatrix}. \tag{7}$$

For states with positive energy, the upper spinor Φ typically exceeds the lower one, X, by a factor c in magnitude – and *vice versa* for states with negative energy.

Within this formulation, we impose the following gauge transformation [5, 6, 13]:

$$\boldsymbol{A} \to \boldsymbol{A} + \nabla\xi \quad \text{and} \quad \varphi \to \varphi - \frac{\partial}{\partial t}\xi \quad \text{with} \tag{8a}$$

$$\xi(\eta) = -\frac{e^2}{2m\omega}\int_{-\infty}^{\eta}[A(\eta')]^2 d\eta', \tag{8b}$$

where φ is the scalar potential. The corresponding kinetic momentum is now

$$\mathbf{d} = \mathbf{p} + e\mathbf{A} + \frac{e^2}{2mc}\mathbf{A}^2\,\hat{\mathbf{k}} \quad . \tag{9}$$

This momentum shift is such that a free, non-quantum mechanical electron starting at zero momentum remains at zero momentum. This applies both to the polarization direction and the propagation direction of the external field, contrary to the usual minimal coupling formulation, in which the canonical momentum acquires a drift velocity along the propagation direction of the pulse.

The gauge transformation of Eqs. (8) leads to the propagation gauge formulation of the Dirac Hamiltonian:

$$H = c\boldsymbol{\alpha}\cdot\mathbf{d} + mc^2\beta + V - \frac{e^2}{2m}\mathbf{A}^2. \tag{10}$$

The much applied dipole approximation, in which the spatial dependence of the vector potential $\mathbf{A}$ is neglected in the minimal coupling formulation, Eq. (4), is in general not applicable in regions where relativistic effects are expected [14]. As mentioned, such an approach is simply too crude as it preclude any magnetic interaction. Within the propagation gauge formulation of Eq. (10), however, the substitution

$$\eta \to \omega t \tag{11}$$

in Eq. (2), constitutes a far less restrictive approximation as it preserves the leading magnetic interaction [5, 6, 13, 15]. In order to clarify this point, we consider the fully non-relativistic Hamiltonian within the propagation gauge formulation [5],

$$H_{\rm NR} = \frac{\mathbf{p}^2}{2m} + V + \frac{e}{m}\mathbf{A}\cdot\mathbf{p} + \frac{e^2\mathbf{A}^2}{2m^2c}\,\hat{\mathbf{k}}\cdot\mathbf{p}, \tag{12}$$

and compare it with the corresponding minimal coupling formulation:

$$H_{\rm NR}^{\rm mc} = \frac{\mathbf{p}^2}{2m} + V + \frac{e}{m}\mathbf{A}\cdot\mathbf{p} + \frac{e^2}{2m}\mathbf{A}^2 \tag{13}$$

It is rather well documented that a first order expansion in the spatial variable of the last term in Eq. (13) constitutes the leading magnetic contribution to the dynamics in the strong field regime [15–20];

$$H_{\rm NR}^{\rm mc} \sim \frac{\mathbf{p}^2}{2m} + V + \frac{e}{m}\mathbf{A}(\omega t)\cdot\mathbf{p} + \frac{e^2}{mc}\mathbf{A}(\omega t)\cdot\mathbf{E}(\omega t)\,\hat{\mathbf{k}}\cdot\mathbf{r}, \tag{14}$$

where the electric field $\mathbf{E} = -\partial_t\mathbf{A}$. This first order contribution corresponds to the radiation pressure induced by the combined action of the external electric and magnetic fields. Now, if we impose the substitution (11) into the Hamiltonian of Eq. (12), we arrive at an interaction form which is equivalent to that of Eq. (14). In the following, we will refer to this formulation of the interaction as the *long wavelength approximation* (LWA). While mathematically equivalent to Eq. (14), the LWA formulation is numerically favourable [5]. This also applies to the corresponding relativistic formulation of the LWA, i.e., Eq. (10) subject to the replacement (11) [13].

A. The transformed Hamiltonian

In a 1950 paper Foldy and Wouthuysen showed how the Dirac equation for a free fermion may be cast into a form which decouples the two spinors of Eq. (7) [21]. By imposing the time-independent unitary transform

$$T = e^S \quad \text{with} \quad S = \frac{1}{2p}\tan^{-1}\left(\frac{p}{mc}\right)\beta\boldsymbol{\alpha}\cdot\mathbf{p} \tag{15}$$

the field free Hamiltonian

$$H_{\rm free} = c\boldsymbol{\alpha}\cdot\mathbf{p} + mc^2\beta \tag{16}$$

was cast into

$$e^S H_{\rm free} e^{-S} = \beta\sqrt{m^2c^4 + p^2c^2}. \tag{17}$$

This is clearly a more intuitive formulation for the relativistic energy than the original formulation, Eq. (16). Moreover, some physical quantities seem to have a more natural interpretation within the frame introduced by the transformation of Eq. (15).

In the following, we will apply the analogous transform to the full Dirac Hamiltonian of Eq. (10), albeit within the LWA. From now on and throughout we take this to be implicit, i.e., "$\mathbf{A}$" will mean "$\mathbf{A}(\omega t)$". We apply the Foldy-Wouthuysen transformation with the momentum $\mathbf{p}$ in Eq. (15) replaced by the momentum $\mathbf{d}$, Eq. (9):

$$T_{\rm PG} = e^{S_{\rm PG}} \quad \text{with} \quad S_{\rm PG} = \frac{1}{2d}\tan^{-1}\left(\frac{d}{mc}\right)\beta\boldsymbol{\alpha}\cdot\mathbf{d} \quad . \tag{18}$$

Now, by following the same derivation as in Ref. [21], the transformation of the two first terms in Eq. (10) is analogous:

$$T_{\rm PG}\left(c\boldsymbol{\alpha}\cdot\mathbf{d} + mc^2\beta\right)T_{\rm PG}^\dagger = \beta\sqrt{m^2c^4 + d^2c^2} \quad . \tag{19}$$

The last term of Eq. (10) is unaltered by the transformation, while the Coulomb potential is affected. Moreover, since the above transformation is time-dependent, the transformed Hamiltonian, H', acquires an additional term:

$$\begin{aligned} H' \;=\; & T_{\rm PG}HT_{\rm PG}^\dagger - i\hbar T_{\rm PG}\frac{d}{dt}T_{\rm PG}^\dagger = \beta\sqrt{m^2c^4 + d^2c^2} \\ & -\frac{e^2}{2m}A^2 + T_{\rm PG}VT_{\rm PG}^\dagger - i\hbar T_{\rm PG}\frac{d}{dt}T_{\rm PG}^\dagger. \end{aligned} \tag{20}$$

In order to determine the last two terms above, we will expand the exponential in the transformation to lowest order in c^{-1},

$$\begin{aligned} S_{\rm PG} &= \frac{1}{2d}\left(\frac{d}{mc} - \frac{1}{3}\left(\frac{d}{mc}\right)^3 + \frac{1}{5}\left(\frac{d}{mc}\right)^5 - ...\right) \\ &\times \beta\boldsymbol{\alpha}\cdot\mathbf{d} = \frac{1}{2mc}\,\beta\boldsymbol{\alpha}\cdot\mathbf{d} + \mathcal{O}(c^{-3}), \end{aligned} \tag{21}$$

and make use of the identity

$$(\boldsymbol{\alpha}\cdot\mathbf{a})(\boldsymbol{\alpha}\cdot\mathbf{b}) = \mathbf{a}\cdot\mathbf{b} + i\boldsymbol{\sigma}\cdot(\mathbf{a}\times\mathbf{b}). \tag{22}$$

With this, it is found that the last term of Eq. (20) reads

$$\begin{aligned} & -i\hbar T_{\rm PG}\frac{d}{dt}T_{\rm PG}^\dagger = \\ & -i\frac{\hbar e}{2mc}\beta\boldsymbol{\alpha}\cdot\mathbf{E}' + \frac{\hbar e}{4m^2c^2}\boldsymbol{\sigma}\cdot(\mathbf{E}'\times\mathbf{d}) + \mathcal{O}(c^{-3}), \end{aligned} \tag{23}$$

where we have introduced

$$\mathbf{E}' = -\frac{d}{dt}\left(\mathbf{A} + \frac{e}{2mc}\mathbf{A}^2\,\hat{\mathbf{k}}\right); \tag{24}$$

it may be seen as the effective electric field corresponding to the external laser field in the propagation gauge.

When it comes to the transformed Coulomb potential, $T_{\rm PG}VT_{\rm PG}^\dagger$, the emerging interaction terms are well known. We will, however, briefly outline the transformation for completeness. Using the Baker-Campbell-Haussdorff formula, we may write

$$\begin{aligned} & e^{S_{\rm PG}}V(\mathbf{r})e^{-S_{\rm PG}} = \\ & V + [S_{\rm PG}, V] + \frac{1}{2}[S_{\rm PG}, [S_{\rm PG}, V]] + \mathcal{O}(c^{-3}). \end{aligned} \tag{25}$$

With this, Eq. (22) and Gauss' law, we arrive at

$$\begin{aligned} T_{\rm PG}VT_{\rm PG}^\dagger = V - i\frac{\hbar e}{2mc}\beta\boldsymbol{\alpha}\cdot\mathbf{E}_C + \frac{\hbar^2 e}{8m^2c^2\varepsilon_0}\rho_C \\ + \frac{\hbar e}{4m^2c^2}\boldsymbol{\sigma}\cdot(\mathbf{E}_C\times\mathbf{d}) + \mathcal{O}(c^{-3}). \end{aligned} \tag{26}$$

where

$$\mathbf{E}_C(\mathbf{r}) = \frac{1}{e}\nabla V(\mathbf{r}) \tag{27}$$

is the static electric field originating from the nucleus and

$$\rho_C(\mathbf{r}) = \varepsilon_0\nabla\cdot\mathbf{E}_C(\mathbf{r}) \tag{28}$$

is its charge distribution. In Eq. (26) it appears in the Darwin term,

$$H_{\rm Darwin} = \frac{\hbar^2 e}{8m^2c^2\varepsilon_0}\rho_C(\mathbf{r}), \tag{29}$$

while the spin-orbit interaction is contained in the last term of Eq. (26).

Gathering all terms from Eqs. (19), (23), (25) and (26), we may write the transformed Hamiltonian Eq. (20) as

$$\begin{aligned} H' = {} & \beta\sqrt{m^2c^4 + \mathbf{d}^2c^2} + V - \frac{e^2}{2m}\mathbf{A}^2 \\ & - i\frac{\hbar e}{2mc}\beta\boldsymbol{\alpha}\cdot\mathbf{E}_{\rm tot} + H_{\rm Darwin} \\ & + \frac{\hbar e}{4m^2c^2}\boldsymbol{\sigma}\cdot(\mathbf{E}_{\rm tot}\times\mathbf{d}) + \mathcal{O}(c^{-3}). \end{aligned} \tag{30}$$

Here we have introduced the "total" electric field:

$$\mathbf{E}_{\rm tot} = \mathbf{E}' + \mathbf{E}_C = \mathbf{E} + \frac{e}{mc}(\mathbf{A}\cdot\mathbf{E})\,\hat{\mathbf{k}} + \mathbf{E}_{\rm C}. \tag{31}$$

B. Decoupling and the semi-relativistic approximation

The only term in Eq. (30) which couples the two components Φ and X of Eq. (7) is the fourth one – the one that contains $\boldsymbol{\alpha}$. We will show that this term is negligible in the softly relativistic region. To this end, we write the Dirac equation with transformed Hamiltonian, Eq. (20), in terms of Φ and X, cf. Eq. (7):

$$
\begin{aligned}
&i\hbar\frac{d}{dt}\begin{pmatrix}\Phi\\ X\end{pmatrix} = H'\begin{pmatrix}\Phi\\ X\end{pmatrix} \quad \text{with}\\
&H' = \\
&\begin{pmatrix} \sqrt{m^2c^4+\mathbf{d}^2c^2}-\frac{e^2\mathbf{A}^2}{2m} & -i\frac{\hbar e}{2mc}\boldsymbol{\sigma}\cdot\mathbf{E}_{\rm tot} \\ i\frac{\hbar e}{2mc}\boldsymbol{\sigma}\cdot\mathbf{E}_{\rm tot} & -\sqrt{m^2c^4+\mathbf{d}^2c^2}-\frac{e^2\mathbf{A}^2}{2m}\end{pmatrix}\\
&+V+H_{\rm Darwin}+\frac{\hbar e}{4m^2c^2}\boldsymbol{\sigma}\cdot(\mathbf{E}_{\rm tot}\times\mathbf{d})+\mathcal{O}(c^{-3}). \quad (32)
\end{aligned}
$$

Following Ref. [12] we introduce the effective, field dressed mass

$$\mu = m\left(1+\frac{e^2}{2m^2c^2}A^2\right) \quad (33)$$

and the momentum-like operator $\mathbf{q}$ defined by

$$\mathbf{q}^2 = \mathbf{p}^2 + 2e\mathbf{A}\cdot\mathbf{p} + \frac{e^2}{mc}\mathbf{A}^2\,\hat{\mathbf{k}}\cdot\mathbf{p}. \quad (34)$$

Note that the field dressed mass μ differs from the rest mass by a term corresponding to the ratio between the "instantaneous" ponderomotive energy U_p, i.e., the ponderomotive energy with cycle-averaging omitted, and the rest mass energy mc^2.

Finally, we shift the energy downwards by the rest mass energy, which allows us to write the first term of Eq. (32) as

$$\begin{pmatrix} \mu c^2\left(\sqrt{1+\frac{\mathbf{q}^2}{\mu^2c^2}}-1\right) & -i\frac{\hbar e}{2mc}\boldsymbol{\sigma}\cdot\mathbf{E}_{\rm tot} \\ i\frac{\hbar e}{2mc}\boldsymbol{\sigma}\cdot\mathbf{E}_{\rm tot} & -\mu c^2\left(\sqrt{1+\frac{\mathbf{q}^2}{\mu^2c^2}}+1\right)\end{pmatrix}.$$

With this, the lower component X, which is small for states with positive energy, obeys the following equation:

$$
\begin{aligned}
&i\hbar\frac{d}{dt}X = \left[i\frac{\hbar e}{2mc}\boldsymbol{\sigma}\cdot\mathbf{E}_{\rm tot}+\mathcal{O}(c^{-3})\right]\Phi+\\
&\left[-\mu c^2\left(\sqrt{1+\frac{\mathbf{q}^2}{\mu^2c^2}}+1\right)+V+H_{\rm Darwin}\right. \quad (35)\\
&\left.+\frac{\hbar e}{4m^2c^2}\boldsymbol{\sigma}\cdot(\mathbf{E}_{\rm tot}\times\mathbf{d})+\mathcal{O}(c^{-3})\right]X \quad .
\end{aligned}
$$

The dominating term acting on X is

$$-\mu c^2\left(\sqrt{1+\frac{\mathbf{q}^2}{\mu^2c^2}}+1\right) = -2\mu c^2 - \frac{\mathbf{q}^2}{2\mu}+\frac{\mathbf{q}^4}{8\mu^3c^2}-... \quad (36)$$

Neglecting all other terms than the leading order contribution of Eq. (36),

$$
\begin{aligned}
&\left[\mu c^2\left(-\sqrt{1+\frac{\mathbf{q}^2}{\mu^2c^2}}-1\right)+V+H_{\rm Darwin}+\right. \quad (37)\\
&\left.\frac{\hbar e}{4m^2c^2}\boldsymbol{\sigma}\cdot(\mathbf{E}_{\rm tot}\times\mathbf{d})+\mathcal{O}(c^{-3})-i\hbar\frac{d}{dt}\right]X\approx -2\mu c^2X,
\end{aligned}
$$

Eq. (35) simplifies to

$$2\mu c^2X = \left[i\frac{\hbar e}{2mc}\boldsymbol{\sigma}\cdot\mathbf{E}_{\rm tot}+\mathcal{O}(c^{-3})\right]\Phi \quad , \quad (38)$$

which, inserted into the equation for the upper component Φ yields

$$
\begin{aligned}
&i\hbar\frac{d}{dt}\Phi = \left[\mu c^2\left(\sqrt{1+\frac{\mathbf{q}^2}{\mu^2c^2}}-1\right)+V+H_{\rm Darwin}\right.\\
&\left.+\frac{\hbar e}{4m^2c^2}\boldsymbol{\sigma}\cdot(\mathbf{E}_{\rm tot}\times\mathbf{d})+\mathcal{O}(c^{-3})\right]\Phi \quad (39)\\
&+\frac{1}{2\mu c^2}(-i^2)\left(\frac{\hbar e}{2mc}\boldsymbol{\sigma}\cdot\mathbf{E}_{\rm tot}+\mathcal{O}(c^{-3})\right)^2\Phi \quad .
\end{aligned}
$$

We now see that the last term on the right hand side is in fact of order c^{-4}. The resulting effective, decoupled Hamiltonian for Φ including terms up to and including second order in $1/c$ thus reads

$$
\begin{aligned}
&H'_\Phi = \mu c^2\left(\sqrt{1+\frac{\mathbf{q}^2}{\mu^2c^2}}-1\right)+V+H_{\rm Darwin}\\
&+\frac{\hbar e}{4m^2c^2}\boldsymbol{\sigma}\cdot(\mathbf{E}_{\rm tot}\times\mathbf{d})+\mathcal{O}(c^{-3}) =\\
&\frac{\mathbf{q}^2}{2\mu}-\frac{\mathbf{q}^4}{8\mu^3c^2}+V+H_{\rm Darwin} \quad (40)\\
&+\frac{\hbar e}{4m^2c^2}\boldsymbol{\sigma}\cdot(\mathbf{E}_{\rm tot}\times\mathbf{d})+\mathcal{O}(c^{-3}) \quad .
\end{aligned}
$$

Note that we here have expanded the kinetic energy operator and retained only the leading and the next-to-leading terms.

Following Ref. [21], the elimination of the term which couples Φ and X, i.e. $-i\hbar e/(2mc)\,\beta\boldsymbol{\alpha}\cdot\mathbf{E}_{\rm tot}$ in Eq. (30), could also be performed by introducing additional unitary transformations.

The first term in the Hamiltonian of Eq. (40),

$$\frac{\mathbf{q}^2}{2\mu} = \frac{\mathbf{p}^2}{2\mu}+\frac{e}{\mu}\mathbf{A}\cdot\mathbf{p}+\frac{e^2}{2m\mu c}\mathbf{A}^2\,\hat{\mathbf{k}}\cdot\mathbf{p} \quad (41)$$

contains the non-relativistic kinetic energy, the usual dipole interaction term and a radiation term induced by the combined electric and magnetic field [5, 6, 15]. These terms coincide with the interaction terms discussed in relation to Eq. (12) – except from the fact that they are modified by the replacement $m\to\mu(t)$; the inertia is effectively increased by the external laser field.

When the vector potential $\mathbf{A}$ of the external field vanishes, the next-to-leading order term in the kinetic energy, $-\mathbf{q}^4/8\mu^3c^2$, coincides with the structure correction

$$E_{\rm kin} = -\frac{\mathbf{p}^4}{8m^3c^2}. \tag{42}$$

The attentive reader may have noticed that there is one familiar term missing in Eq. (40) – the interaction between spin and the external magnetic field. This absence is a direct consequence of the LWA, in which $\nabla \times \mathbf{A} = \mathbf{0}$. While this obviously affect the ability to study of spin dynamics, it does not exclude magnetic interactions all together.

C. Implementation

In our semi-relativistic calculations, we will neglect the spin-degree of freedom entirely for the semi-relativistic calculations. In addition to precluding any investigation of spin dynamics, this could also affect other quantities in which the spin is integrated out. Although we will direct our attention towards ionization probabilities in this work, it is not *a priori* obvious that the neglect of spin is admissible. Moreover, we will neglect the Darwin term, Eq. (29), and the effect the kinetic energy correction, Eq. (42), has on eigen states of the unperturbed Hamiltonian in the semi-relativistic calculations. The adequacy of these approximations will be checked by direct comparison with solutions of the Dirac equation.

This comparison will also serve as a test of the semi-relativistic approximation itself. Specifically, it allows us to gauge wether it is necessary to include the next-to-leading-order term in kinetic energy, i.e., $-\mathbf{q}^4/8\mu^3c^2$ in Eq. (40). For linearly polarized fields, the leading order term, $\mathbf{q}^2/2\mu$, has proven sufficient in calculations pertaining to both the ultra violet [12] and the optical regions [22]. Another work with fields in the X-ray regime, however, demonstrated the need for also including the term proportional to $\mathbf{q}^4$ [23].

Finally, we also solve the completely non-relativistic Schrödinger equation in order to identify relativistic corrections. In summary, these are the dynamical equations we solve:

$$i\hbar\frac{d}{dt}\Psi_{\rm R} = \left[c\boldsymbol{\alpha}\cdot\mathbf{d} + V + mc^2\beta'\right]\Psi_{\rm R} \tag{43a}$$

$$i\hbar\frac{d}{dt}\Psi_{\rm SR} = \left[\frac{\mathbf{q}^2}{2\mu} - \frac{\mathbf{q}^4}{8\mu^3c^2} + V\right]\Psi_{\rm SR} \tag{43b}$$

$$i\hbar\frac{d}{dt}\Psi_{\rm NR} = \left[\frac{\mathbf{q}^2}{2m} + V\right]\Psi_{\rm NR}, \tag{43c}$$

where the Coulomb potential corresponds to a point charge of infinite mass,

$$V(r) = -\frac{e^2}{4\pi\varepsilon_0}\frac{1}{r}, \tag{44}$$

$\mathbf{d}$ is defined in Eq. (9), $\mathbf{q}^2$ is defined in Eq. (34) and $\mu(t)$ is given in Eq. (33). In the case of the Dirac equation, Eq. (43a), the energy has been shifted downwards by mc^2, which, in turn, corresponds to replacing β with

$$\beta' = \begin{pmatrix} 0 & 0 \\ 0 & -2\mathbb{1}_2 \end{pmatrix}. \tag{45}$$

Using a combination of spherical harmonics for the angular part and b-splines for the radial part, we constructed spectral bases by diagonalizing the unperturbed numerical Hamiltonian – both for the relativistic and the non-relativistic case. Eigen states with energies above a certain threshold $E_{\rm threshold}$ were removed from the basis for the non-relativistic and semi-relativistic calculations. In the case of fully relativistic calculations, energies below $-2mc^2 - E_{\rm threshold}$ where also removed.

When solving the semi-relativistic Schrödinger equation, Eq. (43b), we have used the same spectral basis as the non-relativistic one, i.e., we expand $\Psi_{\rm SR}$ in the eigenstates ψ_{n,ℓ,m_ℓ} of the non-relativistic Hamiltonian

$$H_0^{\rm NR} = \frac{\mathbf{p}^2}{2m} + V(r). \tag{46}$$

The spectral basis in which the Dirac equation is solved consists of the eigen states of the time-independent Hamiltonian

$$H_0^{\rm R} = c\boldsymbol{\alpha}\cdot\mathbf{p} + V + mc^2\beta'. \tag{47}$$

Contamination of the spectral basis from spurious states is avoided by using b-splines of order 7 for the radial part of the upper component Φ, cf. Eq. (7), and order 8 for the lower component X [10]. Within these bases, the coupling elements

$$\langle\psi_b|A_i|\psi_a\rangle, \tag{48}$$

where i is x, y and z and $\mathbf{A}$ is $c\boldsymbol{\alpha}$ in the relativistic case and $\mathbf{p}$ in the semi and nonrelativistic cases, are needed in order to calculate the action of the Hamiltonian on the state. The determination of these couplings is facilitated by the Wigner-Eckart theorem, which also enables a sparse representation of the Hamiltonian matrix in our implementation. We maintain the reduced matrix elements, which do not depend on projection quantum numbers, and Clebsch-Gordan coefficients separately. With this, the memory cost scales proportionally to $\ell_{\rm max}$ as opposed to $\ell_{\rm max}^2$, where $\ell_{\rm max}$ is the maximum ℓ included in our truncated angular basis of spherical harmonics. It also presents an excellent opportunity to utilize heterogenous computers efficiently. See Refs. [13, 24, 25] for more details.

In addition to the interaction terms analogous to the non-relativistic ones, the Hamiltonian of Eq. (43b) also feature interaction terms originating from the modified kinetic energy. The semirelativistic Hamiltonian may be written

$$H_{\rm SR} = H_0^{\rm NR} + \left(\frac{1}{2\mu} - \frac{1}{2m}\right)\mathbf{p}^2 + \frac{e}{\mu}\mathbf{A}\cdot\mathbf{p} + \frac{e^2}{2\mu mc}\mathbf{A}^2\,\hat{\mathbf{k}}\cdot\mathbf{p} - \frac{\mathbf{q}^4}{8\mu^3c^2}. \tag{49}$$

The coupling elements induced by the relativistic mass correction in kinetic energy, which is proportional to $\mathbf{p}^2$, are calculated via the Coulomb potential as

$$\langle\psi_{n',\ell',m'_\ell}|\mathbf{p}^2|\psi_{n,\ell,m_\ell}\rangle = 2m\langle\psi_{n',\ell',m'_\ell}|\left(H_0^{\rm NR}-V\right)|\psi_{n,\ell,m_\ell}\rangle, \quad (50)$$

which is convenient since the $H_0^{\rm NR}$ operator is diagonal and $V(r)$ is spherically symmetric;

$$\langle\psi_{n',\ell',m'_\ell}|H_0|\psi_{n,\ell,m_\ell}\rangle = \varepsilon_{n,\ell}\delta_{n,n'}\delta_{\ell,\ell'}\delta_{m_\ell,m'_\ell} \quad \text{and} \quad (51a)$$

$$\langle\psi_{n',\ell',m'_\ell}|V|\psi_{n,\ell,m_\ell}\rangle = \langle\psi_{n',\ell',m'_\ell}|V|\psi_{n,\ell,m_\ell}\rangle\delta_{\ell,\ell'}\delta_{m_\ell,m'_\ell}. \quad (51b)$$

Here $\varepsilon_{n,\ell}$ are the eigen energies of the numerical representation of $H_0^{\rm NR}$; they include the energies of both bound states and box-normalized pseudo continuum states. With the coupling elements (48) of each momentum component, the dipole interaction $e/\mu\,\mathbf{A}\cdot\mathbf{p}$ and the radiation pressure $e^2/(2\mu mc)\,\mathbf{A}^2\,\hat{\mathbf{k}}\cdot\mathbf{p}$ is implemented. This also allows us to calculate the action of $\mathbf{q}^2$ on the wave function, which, in turn, allows us to determine the action of $\mathbf{q}^4$ by applying $\mathbf{q}^2$ to the wave function twice. As mentioned, this approach imposes, in principle, an error. In our semirelativistic calculations we take our initial state to be a non-relativistic bound state of $H_0^{\rm NR}$. Since the kinetic energy correction, Eq. (42), is part of the $\mathbf{q}^4$ interaction, it will impose a perturbation on the initial state which prevails even when there is no external field. For the case of hydrogen, however, it is reasonable to assume that this error may be neglected. Numerical checks confirm that this is indeed admissible. The issue would, however, be problematic for highly charged ions.

The fact that we expand our wave function in eigenstates of the unperturbed Hamiltonians renders the calculation of ionization probabilities straight forward; it is simply one minus the sum of the populations of all bound states. The populations of the box-normalized pseudo-continuum states, in turn, can be used to interpolate the energy distribution of the ionized electron. In doing so, the proper normalization factor, i.e., the density of states, is imposed and contributions from the various ℓ, m_ℓ channels are added incoherently.

The time-propagation is achieved using a second order magnus propagator approximated by means of a Krylov subspace technique [26–28]. In our simulations we have applied a $\sin^2$ envelope function, and the carrier envelope phase $\phi = 0$. The laser field is polarized in the x, y plane, $\hat{\mathbf{a}}_1 = \hat{\mathbf{x}}$ and $\hat{\mathbf{a}}_2 = \hat{\mathbf{y}}$, which corresponds to propagation along the z axis, $\hat{\mathbf{k}} = \hat{\mathbf{z}}$, cf. Eq. (1).

III. RESULTS AND DISCUSSION

As mentioned, the semi-relativistic approach has previously been tested by direct comparison with solutions of the Dirac equation for cases involving linear polarization [12, 22, 23]. We will here demonstrate its adequacy for elliptic polarization. The results presented in Fig. 1 display the total ionization yields for a hydrogen atom in the ground state exposed to a short, intense laser pulse in the ultra violet region. Specifically, the central angular frequency of the field is $\omega = 3.5$ a.u. and the pulse duration T corresponds to 15 optical cycles; $T = 15 \cdot 2\pi/\omega$.

Converged results where obtained using an expansion in 500 b-splines extending up to $r_{\rm max} = 150$ a.u. The expansion in partial waves was truncated at $\ell_{\rm max} = 40$, and the energy truncation was set to $E_{\rm threshold} = 200$ a.u. In the case of fully relativistic calculations, a numerical time step corresponding to 2000 steps per optical cycle was applied at the highest field intensities. A somewhat longer time step was sufficient in the case of semi-relativistic and non-relativistic calculations.

The upper panel shows the ionization probability as a function of peak electric field strength E_0 for various ellipticities δ, cf. Eq. (1). It is clearly seen that the ionization probability is very weakly dependent on ellipticity, which is hardly surprising given the isotropic shape of the ground state wave function. The relativistic correction to the ionization probability is more interesting in this regard. The difference between the ionization probability as predicted by relativistic Dirac equation, Eq. (43a) and the non-relativistic results of the Schrödinger equation, Eq. (43c), are shown in the lower panel of Fig. 1. We have also included the corresponding relativistic correction obtained using the semirelativistic Schrödinger equation (43b) instead of the Dirac equation. We see a small but noticeable relativistic correction. We also see quantitative agreement between the relativistic corrections provided by the fully relativistic calculations and the semirelativistic ones. Albeit weaker, the agreement is still reasonable when only the leading order in kinetic energy is retained. This is particularly so for higher field strengths. This, in turn, may be understood from the fact that the relativistic mass $\mu(t)$ increases with increasing field strength. As a consequence, the approximation

$$\mu c^2\left(\sqrt{1+\left(\frac{\mathbf{q}}{\mu c}\right)^2}-1\right) \approx \frac{\mathbf{q}^2}{2\mu} \quad (52)$$

becomes increasingly justified.

The relativistic correction is seen to be negative for all intensities studied here. This is in agreement with previous works [12, 22, 24], and it can be understood from the fact that the increased inertia acquired by the electron renders it slightly more stable against ionization.

The lower panel of Fig. 1 shows that the overall relativistic correction is larger for linear polarization ($\delta = 0$), it tends to decrease with increasing ellipticity towards circular polarization ($\delta = 45°$). This is not surprising considering the fact that, while the *average* velocity imposed on the electrons by the external field is independent of ellipticity, the *peak* velocity is higher for linear polarization. Thus, a linearly polarized field pushes the electron deeper into the relativistic region than a circularly polarized field of the same intensity would.

Having validated the semi-relativistic approximation we will resort to this approach in the remainder of this paper, i.e., we will consistently solve Eq. (43b) instead of Eq. (43a). As mentioned, this is convenient since the numerical solution of a Schrödinger-type equation such as this one is far less involved than the corresponding Dirac equation.

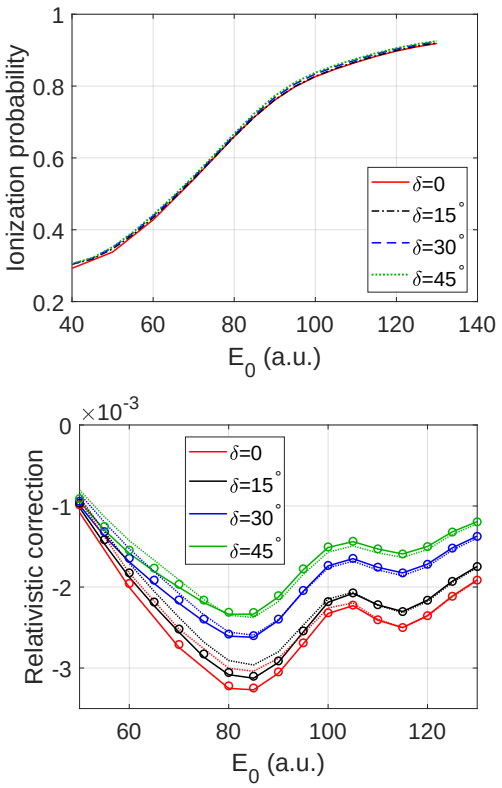

FIG. 1: The upper panel shows the total ionization probability for a hydrogen atom as a function of peak electric field strength E_0 and ellipticity δ. The system is initially prepared in the ground state and the laser pulse has central frequency of $\omega = 3.5$ a.u. and a duration corresponding to 15 optical cycles. A very weak dependence on the ellipticity is seen. The lower panel displays the relativistic correction to the ionization yield. Here, the full curve shows the difference in ionization probability as predicted by the Dirac and the Schrödinger equation. The dashed curves shows the relativistic correction as predicted by the semi-relativistic approach with truncation at lowest order in the kinetic energy operator, Eq. (52), while the circles corresponds to calculations in which the next-to-leading order is retained, cf. Eq. (43b).

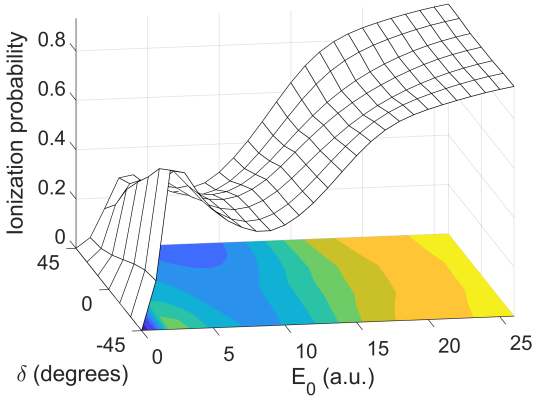

FIG. 2: The ionization probability as a function of peak electric field strength E_0 and ellipticity δ, cf. Eq. (1). The initial state has (non-relativistic) quantum numbers $n = 2$, $\ell = m_\ell = 1$, and the laser pulse has $\omega = 1$ a.u. and a duration of 15 optical cycles.

It is to be expected that with a non-isotropic initial state, the ionization probability will feature a much stronger δ-dependence than the one seen in ionization from the ground state. Fig. 2 demonstrates that this is indeed the case when we take our initial state to be the excited state with $n = 2$, $\ell = m_\ell = 1$. The figure shows the ionization yield as a function of E_0 and δ. In this case, the central angular frequency of the external field is $\omega = 1$ a.u. while the pulse duration remains 15 optical cycles. Converged results where achieved with $\ell_{\max} = 25$, 2000 b-splines per angular symmetry and $r_{\max} = 1000$. Weaker fields allowed for a slightly lower value for $r_{\max}$. We propagated the wave function using 200 steps per optical cycle, and the energy-truncation was $E_{\text{threshold}} = 100$ a.u.

The ionization probability is seen to feature a pronounced stabilization peak around $E_0 \sim 2.5$ a.u. [29]. The δ-dependence is particularly strong at this peak. As in the case of Ref. [30], the ionization yield tends to be lowest for circularly polarized fields rotating opposite to the z-axis ($\delta = 45°$), i.e., against the angular momentum of the initial state, and highest for co-rotating circular fields ($\delta = -45°$). Beyond the stabilization peak, the δ dependence weakens, and the ionization probability is virtually δ independent as the system approaches saturation.

Also in the case pertaining to Fig. 2, we do see certain relativistic corrections. These are demonstrated in Fig. 3. As in the case showed in the lower panel of Fig. 1, the correction is highest in magnitude for linear polarization. Beyond the stabilization peak, it tends to be slightly higher for contra-rotating than co-rotating polarization. This may appear somewhat counter intuitive; one would typically expect to see higher relativistic corrections in the case of a co-rotating field.

For all ellipticities, the relativistic correction is largest in magnitude for E_0 values in the vicinity of 15 a.u., and also here it decreases as the system approaches saturation.

It is interesting to note that the relativistic correction shown in Fig. 3 is not strictly negative. In fact, for comparatively moderate field strengths, E_0 between 2 a.u. and 10 a.u., relativity tend to provide a slight enhancement of ionization. The regions in which the relativistic correction is positive does, to a large extent, coincide with the regions in which the ionization probability is decreasing with intensity. This is illustrated in Fig. 4.

This coincidence suggests that relativity amounts to an effective reduction in field strength at these intensities. This, in turn, is concordant with the fact that the dipole interaction term $e/m\,\mathbf{A}\cdot\mathbf{p}$ is replaced by $e/\mu\,\mathbf{A}\cdot\mathbf{p}$ in the semirelativistic approximation. However, for these field strengths, the reduction in effective field strength, $E_0 \to m/\mu E_0$, is too small to account for the full correction. Instead, we consider the full

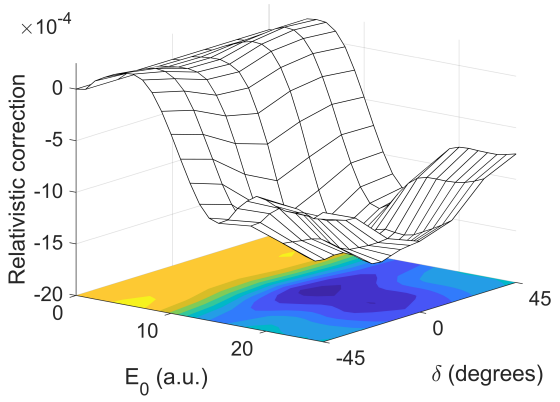

FIG. 3: The relativistic correction to the ionization probability displayed in Fig. 2 as a function of peak electric field strength E_0 and ellipticity δ. Specifically, it shows the difference between the ionization probability predicted by the semirelativistic approach, Eq. (43b) and the non-relativistic one, Eq. (43c).

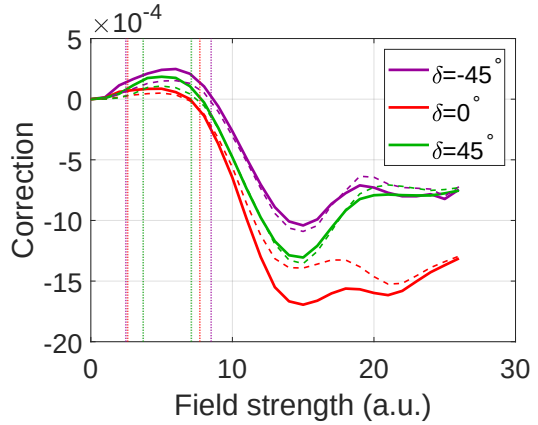

FIG. 4: As in Fig. 3, this plot shows the relativistic correction to the total ionization yield. In this case it is only displayed for three ellipticities, namely co-rotating circular polarization ($\delta = -45°$), linear polarization ($\delta = 0$) and contra-rotating circular polarization ($\delta = 45°$). As in the lower panel of Fig. 1, the dashed curves correspond to relativistic corrections predicted with only the leading term in the kinetic energy operator retained, cf. Eq. (52). The dotted vertical lines indicate the respective intervals in which the ionization probability is a decreasing function of intensity.

Hamiltonian of Eq. (43b) written out explicitly:

$$H_{\rm SR} = \frac{\mathbf{p}^2}{2m} - \frac{\mathbf{p}^4}{8m^3c^2} + V + \frac{e^2}{2m^2c}\mathbf{A}^2\,\hat{\mathbf{k}}\cdot\mathbf{p} + \frac{e}{m}\left(1 - \frac{e^2\mathbf{A}^2 + \mathbf{p}^2}{2m^2c^2}\right)\mathbf{A}\cdot\mathbf{p} - \frac{e^2}{4m^3c^2}\left(\mathbf{A}^2\mathbf{p}^2 + 2\,(\mathbf{A}\cdot\mathbf{p})^2\right) + \mathcal{O}(c^{-3}). \qquad (53)$$

This expression is identical to Eq. (13) of Ref. [31] – apart from the anti-commutators between $\mathbf{p}$ and $\mathbf{A}$ imposed in the latter expression, which is not restricted to the LWA. We identify an additional term which also supports the notion of an effective reduction in field strength, namely the relativistic correction term $-e\mathbf{p}^2/(2m^3c^2)\,\mathbf{A}\cdot\mathbf{p}$. As this term is linear in $\mathbf{A}$, it is reasonable to assume that also this term constitutes a significant correction at these comparatively moderate field strengths, as supported by a comparison between the dashed and the full curves in Fig. 4.

In Fig. 5 we display photoelectron spectra obtained with peak electric field strength $E_0 = 20$ a.u. These calculations require higher resolution in terms of partial waves than what is needed for calculating total ionization probabilities. In this particular case, convergence was achieved with $\ell_{\rm max} = 35$. Moreover, we have imposed a complex absorbing potential near the edge of the numerical grid for these calculations. Fully relativistic calculations indicated that the semirelativistic calculations indeed produced the correct relativistic modifications also in this case. However, convergence issues related to the numerical solution of the Dirac equation, Eq. (43a), hindered establishing a fully quantitative agreement.

The field strength $E_0 = 20$ a.u. corresponds to an intensity well beyond the stabilization peak, in which the multi photon peaks are not expected to be prominent [32–34]. Thus, it should come as no surprise that the spectra are dominated by low energy photo electrons. Still, we may make out some multi photon peaks for circular polarization. For $E_0 = 20$ a.u., the relativistic correction tends to reduce the total ionization yield. Accordingly, the over all relativistic correction is negative, as demonstrated in the lower panel of Fig. 5. However, it is not negative for all energies; as it turns out, relativistic corrections impose a slight enhancement just above threshold for circular polarizations. And it does so to a larger extent in the case of co-rotating polarization than for a contra-rotating field. In other words, there seems to be two competing relativistic corrections; one which enhances ionization at low energies and another which diminishes it at higher photo electron energies. The latter is consistent with the discussion pertaining to Fig. 4. Supported by the expression for the modified dipole interaction, i.e., the second last term in Eq. (53), increased inertia may, to some extent, be seen as an effective reduction in field strength.

Thus, it would seem reasonable to attribute the relativistic enhancement seen for low-energy photo electrons exposed to circular polarization to the last term Eq. (53). This interaction term features a modification of the kinetic energy term, $e^2\mathbf{A}^2/(2m^3c^2)\,\mathbf{p}^2$. As $\langle\mathbf{p}^2\rangle$ typically is larger for co-rotating than contra-rotating circular polarization, this may explain why the enhancement is more pronounced in the former case. Note that both effects, the enhanced ionization probability near zero energy and reduced ionization at higher energies, are more pronounced for co-rotating than contra rotating fields. In light of this, the fact that relativistic corrections to the *total* ionization probability tends to be smaller in magnitude in the co-rotating case than the contra-rotating case appears less counter-intuitive. Although both the relativistic effects discussed above are stronger for co-rotating polarization, they add up to a total correction which is more moderate than what is seen for contra-rotating polarization.

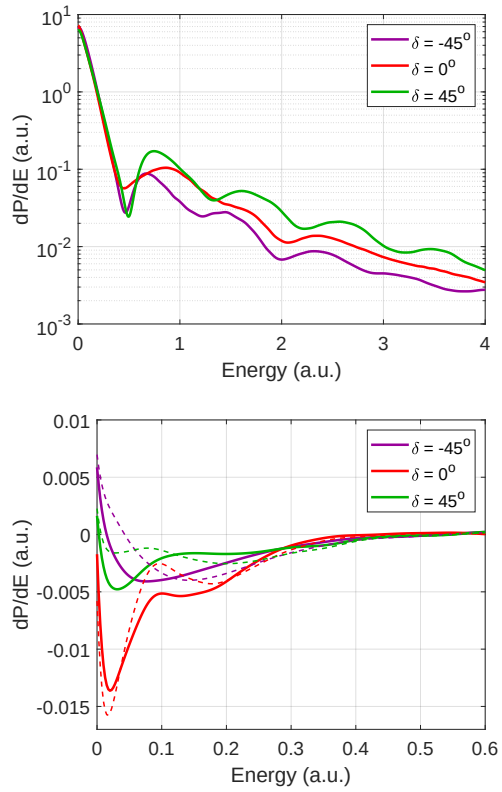

FIG. 5: The upper panel shows the energy differential ionization probability for co-rotating ($\delta = -45^\circ$), linear ($\delta = 0$) and contra-rotating ($\delta = 45^\circ$) polarization for the same system as in Fig. 2. The peak electric field strength is $E_0 = 20$ a.u. The spectra are plotted with a logarithmic y axis. The lower panel shows the relativistic corrections to the spectra on a linear scale. The dashed curves corresponds to lowest order truncation in kinetic energy, Eq. (52).

IV. CONCLUSIONS

We have validated the semirelativistic approach to photo ionization for strong electromagnetic fields of general ellipticity in the ultra violet region and applied it to study photo ionization of a hydrogen atom initially excited to the $n = 2$, $\ell = m_\ell = 1$ state. A strong dependence on ellipticity near the stabilization peak was found; co-rotating circular polarization provided significantly higher ionization than contra-rotating polarization.

Certain relativistic corrections were also observed. In general, the magnitude of the correction was highest for linear polarization, for which the peak electric field strength penetrates deeper into the relativistic region. For most field strengths, relativity tends to stabilize the system slightly against ionization – in accordance with the notion of increased inertia induced by the laser pulse. However, in the regions in which ionization probability is decreasing with increasing intensity, a relativistic *enhancement* of ionization was seen. This enhancement was also interpreted as a consequence of an effective reduction in the laser intensity.

We also presented photoelectron spectra for an intensity well beyond stabilization. These spectra demonstrated that multi photon ionization is suppressed at these intensities and that photo electrons, for all ellipticities, tend to come out with very low energy. While relativistic effects over all tend to stabilize the atom against ionization, a certain enhancement was seen for low-energy photo electrons exposed to circularly polarized fields.

Acknowledgements

Simulations have been performed on the supercomputer Saga, with computational time provided by UNINETT Sigma2 – the National Infrastructure for High Performance Computing and Data Storage in Norway (Project No. NN9417K). Constructive discussions with prof. Morten Førre are gratefully acknowledged.

[1] A. D. DiChiara, I. Ghebregziabher, R. Sauer, J. Waesche, S. Palaniyappan, B. L. Wen, and B. C. Walker, Phys. Rev. Lett. **101**, 173002 (2008).
[2] H. Yumoto, H. Mimura, T. Koyama, S. Matsuyama, K. Tono, T. Togashi, Y. Inubushi, T. Sato, T. Tanaka, T. Kimura, et al., Nat. Photon **7**, 43 (2013).
[3] H. Yoneda, Y. Inubushi, M. Yabashi, T. Katayama, T. Ishikawa, H. Ohashi, H. Yumoto, K. Yamauchi, H. Mimura, and H. Kitamura, Nat. Commun **5**, 5080 (2014).
[4] A. Di Piazza, C. Müller, K. Z. Hatsagortsyan, and C. H. Keitel, Rev. Mod. Phys. **84**, 1177 (2012).
[5] M. Førre and A. S. Simonsen, Phys. Rev. A **93**, 013423 (2016).
[6] A. S. Simonsen and M. Førre, Phys. Rev. A **93**, 063425 (2016).
[7] D. A. Telnov and Shih-I Chu, Phys. Rev. A **102**, 063109 (2020).
[8] I. A. Ivanov, Phys. Rev. A **91**, 043410 (2015).
[9] V. M. Shabaev, I. I. Tupitsyn, V. A. Yerokhin, G. Plunien, and G. Soff, Phys. Rev. Lett. **93**, 130405 (2004).
[10] C. Froese Fischer and O. Zatsarinny, Computer Physics Communications **180**, 879 (2009), ISSN 0010-4655.
[11] F. Fillion-Gourdeau, E. Lorin, and A. D. Bandrauk, Phys. Rev. A **85**, 022506 (2012).
[12] T. Kjellsson Lindblom, M. Førre, E. Lindroth, and S. Selstø, Phys. Rev. Lett. **121**, 253202 (2018).
[13] T. Kjellsson, M. Førre, A. S. Simonsen, S. Selstø, and E. Lindroth, Phys. Rev. A **96**, 023426 (2017).
[14] H. R. Reiss, Phys. Rev. A **63**, 013409 (2000).
[15] J. R. Vázquez de Aldana, N. J. Kylstra, L. Roso, P. L. Knight, A. Patel, and R. A. Worthington, Phys. Rev. A **64**, 013411 (2001).
[16] A. Bugacov, M. Pont, and R. Shakeshaft, Phys. Rev. A **48**, R4027 (1993).
[17] K. J. Meharg, J. S. Parker, and K. T. Taylor, J. Phys. B **38**, 237

(2005).
[18] H. Bachau, M. Dondera, and V. Florescu, Phys. Rev. Lett. **112**, 073001 (2014).
[19] M. Førre, Phys. Rev. A **74**, 065401 (2006).
[20] M. Førre and A. S. Simonsen, Phys. Rev. A **90**, 053411 (2014).
[21] L. L. Foldy and S. A. Wouthuysen, Phys. Rev. **78**, 29 (1950).
[22] T. Kjellsson Lindblom, M. Førre, E. Lindroth, and S. Selstø, Phys. Rev. A **102**, 063108 (2020).
[23] M. Førre, Phys. Rev. A **99**, 053410 (2019).
[24] T. Kjellsson, S. Selstø, and E. Lindroth, Phys. Rev. A **95**, 043403 (2017).
[25] T. Kjellsson Lindblom, Ph.D. thesis, Stockholm University, Dept. of Physics (2017).
[26] M. Hochbruck and C. Lubich, SIAM J. Numer. Anal. **41**, 945 (2003).
[27] S. Blanes, F. Casas, J. Oteo, and J. Ros, Physics Reports **470**, 151 (2009).
[28] R. Beerwerth and H. Bauke, Comput. Phys. Comm. **188**, 189 (2015).
[29] M. Gavrila, J. Phys. B **35**, R147 (2002).
[30] S. Askeland, S. A. Sørngård, I. Pilskog, R. Nepstad, and M. Førre, Phys. Rev. A **84**, 033423 (2011).
[31] M. Førre and S. Selstø, Phys. Rev. A **101**, 063416 (2020).
[32] M. Førre, S. Selstø, J. P. Hansen, and L. B. Madsen, Phys. Rev. Lett. **95**, 043601 (2005).
[33] M. Førre, J. P. Hansen, L. Kocbach, S. Selstø, and L. B. Madsen, Phys. Rev. Lett. **97**, 043601 (2006).
[34] K. Toyota, O. I. Tolstikhin, T. Morishita, and S. Watanabe, Phys. Rev. Lett. **103**, 153003 (2009).